Int. J. Hyperthermia, June 2010; 26(4): 338–346

informa
healthcare

RESEARCH ARTICLE

Temperature monitoring utilising thermoacoustic signals during pulsed microwave thermotherapy: A feasibility study

CUNGUANG LOU & DA XING

MOE Key Laboratory of Laser Life Science & Institute of Laser Life Science, College of Biophotonics, South China Normal University, Guangzhou, China

(Received 30 September 2009; Revised 31 December 2009; Accepted 4 January 2010)

Abstract
Thermotherapy is an attractive alternative to surgery and radiation therapy because of its ability to locally kill tumours while preserving surrounding normal tissues. An important part of successful thermotherapy is real-time temperature monitoring to control the area being heated while protecting normal tissue. The pulsed microwave absorbed by biological tissue can excite ultrasonic waves via thermoelastic expansion, while the magnitude of the acoustic signal is temperature-dependent. The goal of this work is to develop an approach for treatment monitoring of thermotherapy. The pulsed microwave serves as an acoustic excitation source as well as heating source. Temperature is real-time monitored by the magnitude of the thermoacoustic signals. Experiments were conducted in phantoms and fresh *ex vivo* tissues, an accuracy of 0.2°C was obtained. This approach has the potential to be developed into a viable alternative to current clinical temperature monitoring device for microwave thermotherapy.

Keywords: *thermoacoustic signals, temperature monitor, pulsed microwave, thermotherapy*

Introduction

In recent years, microwave thermotherapy (MT) has been an important treatment in oncology. It has been used successfully in biological therapy for breast cancer, prostate cancer, head and neck cancer [1–3]. One of the most significant barriers to wider acceptance of thermotherapy has been the lack of adequate temperature monitoring method which has limited the optimization and control of the treatment. There are invasive techniques for monitoring tissue temperature as well as non-invasive techniques such as magnetic resonance imaging (MRI), computed tomography (CT), ultrasound (US) and microwave tomographic imaging [4–9]. In invasive methods, semiconductor thermistor or thermocouple components are inserted into the tumour centre. In order to eliminate the influence of electromagnetic interference, temperature measurements should be conducted during a brief interruption of heating. Moreover, it causes pain as well as creating the possibility of cancer transfer. In order to overcome these shortcomings, novel non-invasive temperature measurement processes with relatively high precision should be vigorously explored and researched as a replacement.

The required accuracy and spatial resolution can be achieved by MRI. However, MR temperature monitoring has its drawbacks. These include motion artifacts which can be substantial over a lengthy heating procedure, integration challenges associated with the therapy device, and cost [8, 9]. Ultrasound has been successively used in the diagnosis and treatment of malignant tumours due to its non-invasive and non-ionising characteristics [10, 11]. Several ultrasound approaches [12–15] have also been investigated as thermotherapy monitoring candidates because of the significant temperature dependence of their associated properties – speed of sound, sound attenuation, backscattered power, and thermal expansion, but neither has been

Correspondence: Da Xing, PhD, Professor, MOE Key Laboratory of Laser Life Science and Institute of Laser Life Science, College of Biophotonics, South China Normal University, Guangzhou 510631, China. Tel: +86-20-8521-0089. Fax: +86-20-8521-6052. E-mail: xingda@scnu.edu.cn

ISSN 0265–6736 print/ISSN 1464–5157 online
DOI: 10.3109/02656731003592035

implemented in the clinic so far due to the limited resolution and accuracy [13]. One of these techniques is based on tracking the echo-shift in the time-domain, and differentiating the time-shift to obtain a temperature profile. However, only the average temperature of a specific range can be obtained, which makes it have relatively poor spatial resolution [14]. In addition, the measurement process is often influenced by the organ motion and is therefore not suitable for clinical applications. Thermotherapy temperature can also be monitored by sound attenuation, which is known to significantly change when exposed to high temperatures [16, 17]. The challenge here is that accurate extraction of attenuation coefficient from echo wave is very difficult. Moreover, the increased rate of backscatter and attenuation are only obvious at high temperature (55°C or higher). Therefore, the method of measuring acoustic attenuation is well suitable for monitoring of hyperthermia, but it does not apply to thermotherapy.

The thermoacoustic (TA) effect refers to the generation of acoustic waves by electromagnetic (EM) irradiation such as optical or microwave/radio frequency waves. In the past ten years, thermoacoustic tomography (TAT) using pulsed EM excitation has undergone tremendous growth [18–20]. Energy deposition inside biological tissue through the absorption of incident EM pulses will create a transient temperature rise in the order of 10 mk. In the thermoelastic mechanism of acoustic generation, a sound or stress wave is produced as a consequence of the expansion induced by the temperature variation [21]. We found thermoacoustic signals are temperature dependent, which is an ideal characteristic for use in monitoring biological tissue temperature. This paper presents a study on pulsed microwave-induced thermoacoustic signals with the intent of monitoring tumour tissue temperature during thermotherapy. The pulsed microwave serves as an acoustic excitation source as well as heating source, and experiments were performed on phantoms and fresh ex vivo tissue samples. The results indicate that the presented method is feasible and sufficiently sensitive to monitor tissue temperature. Moreover, the thermotherapy ability of pulsed microwaves means it can be used to construct a combined therapy/monitoring system.

Methods and materials

Thermoacoustic theory

The conditions of stress confinement have to be met in thermoacoustic wave generation. In soft tissues, the EM energy is deposited within a relatively short time, hence the thermal diffusion effect is usually negligible. Under the afore-mentioned conditions, the initially excited acoustic stress or pressure is determined by the local EM absorption. In response to a heat source without considering thermal diffusion and kinematical viscosity, the pressure at position r and time t in an acoustically homogeneous medium obeys the following wave equation: [22]

$$\nabla^2 \mathrm{P}(r,t) - \frac{1}{C_0^2}\frac{\partial^2}{\partial t^2}\mathrm{P}(r,t) = -\frac{\beta}{C_p}\frac{\partial}{\partial t}\mathrm{H}(r,t), \qquad (1)$$

where β is the isobaric volume expansion coefficient, C_0 is the speed of sound, C_p is the heat capacity, and $\mathrm{H}(r,t)$ is the heating function defined as the thermal energy per unit time and unit volume deposited by the energy source.

In general, the solution of Equation 1 in the time domain can be expressed by [23, 24]:

$$p(r,t) = \frac{\beta}{4\pi \mathrm{C_p}} \iiint \frac{d^3 r'}{|r-r'|} \left.\frac{\partial \mathrm{H}(r',t')}{\partial t'}\right|_{t'=t-\frac{|r-r'|}{c}}. \qquad (2)$$

The heating function can be written as the product of a spatial absorption function and a temporal illumination function:

$$\mathrm{H}(r,t) = A(r)I(t). \qquad (3)$$

Particularly $I(t) = \delta(t)$ under the conduction of thermal confinement, subject to zero-initial-value conditions $\mathrm{P}(r,0) = 0$ and $\frac{\partial}{\partial t}\mathrm{P}(r,0) = 0$ result in the following equation [25–27]:

$$\mathrm{P(z)} = (\beta \mathrm{C}^2/\mathrm{C_p})\mu_a \mathrm{H} = \Gamma \mu_a \mathrm{H(z)} = \Gamma \mu_a \mathrm{H}_0 e^{(-\mu_a z)} \qquad (4)$$

The expression of $\beta C^2/C_p$ represents the Grüneisen parameter (Γ) that equals to 0.11 for water and 0.23 for muscular at room temperature. $e^{(-\mu_a z)}$ represents the attenuation of the electromagnetic field strength as a function of distance from the radiator (its impact was ignored due to the signals which were captured from the same depth).

The Grüneisen parameter is a dimensionless, temperature-dependent factor which is related to the thermal and bulk properties of the medium. Γ is proportional to the fraction of thermal energy converted into mechanical stress. The thermal expansion coefficient (β) defines the fractional changes in the volume of a material with temperature – normally its value increases almost linearly with temperature except for the lowest temperatures [28–30]. There is a linear relationship between tissue thermal expansion coefficient and temperature between 25°C and 55°C [31, 32], thus Γ can be expressed by the equation:

$$\Gamma = \mathrm{A} + \mathrm{B} * \mathrm{T} \qquad (5)$$

where A, B are constants and T is the temperature measured in °C. The absorption coefficient can be expressed as:

$$\mu_\alpha = \omega \sqrt{\frac{\mu\varepsilon}{2}\left[\sqrt{1+\left(\frac{\sigma}{\omega\varepsilon}\right)^2}-1\right]} \tag{6}$$

where ω is the angular frequency, μ is the permeability, ε is the permittivity, and σ is the conductivity. The complex dielectric properties of tissues determine the propagation and absorption distribution of microwaves. Several investigators have shown that the electrical conductivity of materials is temperature-dependent [32]. The temperature rise causes an increase in the electrical conductivity, which will also lead to change in thermoacoustic signals.

According to the above equations, the thermoacoustic pressure is correlated with the conductivity and Γ, and it can be written in the following forms:

$$\mathrm{P}(z_0) = (\mathrm{A} + \mathrm{B} * \mathrm{T})\mathrm{P}_0, \tag{7}$$

where P_0 is the thermoacoustic pressure generated at baseline temperature, z_0 is the depth. The equation demonstrates that the thermoacoustic pressure is directly proportional to temperature where its variation is the reaction of sample thermodynamic parameter changes with heat. According to Sigrist's study [24] for bipolar thermoacoustic signals, both the positive and negative extrema were proportional to temperature while the peak–peak value was used in this study to define the amplitude of thermoacoustic signal. On the basis of the theoretical description, after establishing the linear regression equation of thermoacoustic pressure with temperature, the actual temperature corresponding to recorded signals can be calculated.

The measurement accuracy of the present method was compared with the ultrasound method which is based on measuring change in sound speed. According to the previous study [14, 15], the variation in the acoustic transit time through a medium changes with temperature, and it can be obtained by the equation:

$$\Delta t = t(\mathrm{T}_0 + \Delta\mathrm{T}) - t(\mathrm{T}_0). \tag{8}$$

The differential can be calculated using a cross-correlation algorithm. Therefore, the change of the sound speed can be retrieved easily and the temperature rise can be calculated from the velocity change.

Experimental setup

A block diagram of the experimental setup is shown in Figure 1. A pulsed 6 GHz microwave generator (BW-6000HPT, Xian, China) was employed as the excitation source. The microwave was delivered to the sample through a rectangular waveguide with an opening of $34 \times 15\,\mathrm{mm}^2$ and TE10 mode. A clock signal provided by a function generator was used for triggering the microwave generator. The peak pulsed power was 300 KW which could be adjusted by voltage regulation, and the average output power was 9 W when the pulse repetition frequency (PRF) measured 50 Hz. The great advantage of the microwave generator is that its PRF and pulse width can be freely adjusted, hence power regulation can be obtained by controlling the pulse. The PRF has an adjustable range of 1 Hz-500 Hz and the pulse duration has a span from 0.35 μs and 1.2 μs.

The acquisition system utilised in the experiment was based on an acoustic transducer and oscilloscope. A piezoelectric transducer (Doppler, Guangzhou, China, Central frequency: 2.5 MHz) and a needle polyvinylidene fluoride (PVDF) hydrophone (Precision Acoustics, Dorchester, UK. Sensitivity: 850 *nV/Pa*) were employed to receive the time-resolved acoustic signals. They are subsequently amplified (Precision Acoustics) with gain of 55 dB and recorded by a digital oscilloscope (TDS3032B, Tektronix, Oregon, USA) at a sampling rate of 250 MS/s. The thermoacoustic signal was averaged for 256 times to improve the signal-to-noise ratio (SNR). The averaging and recording time for one measurement was 12 s.

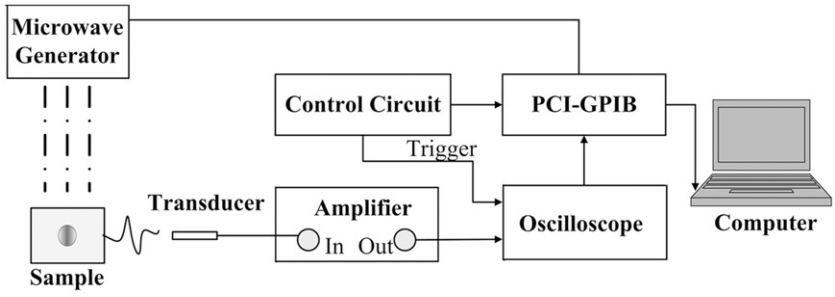

Figure 1. An experimental set-up schematic of pulsed microwave thermotherapy and in situ temperature monitoring system. The coupling medium between sample and transducer is oil in a plastic bag.

The data collection was controlled by a GPIB card (PCI-GPIB, National Instruments, Austin, USA) and the control modules were written using the Labview programming language (National Instruments).

Experimental materials and procedure

Prior to temperature monitoring studies, experiments were performed with water as a sample to investigate the relationship between temperature and thermoacoustic pressure. The water was heated in a tank and pumped to the location of the microwave beams, the thermoacoustic signal was recorded with time as the temperature rise. The actual temperature of the sample was also monitored by digital thermometer (51-II, Fluke, Everett, WA, USA) with an accuracy of 0.1°C.

In order to evaluate the biomedical performance of this method, three independent experiments with different PRF were performed on pieces of freshly excised porcine muscle tissue. The approximate dimensions of the muscle were 15 mm × 10 mm, and the thickness of the muscle was 10 mm. A piece of muscle tissue was used for each experiment and the measurement was repeated twice. For each PRF, the sample was first heated by the pulsed microwave, and thermoacoustic signal was recorded with time as the temperature increased. Then the sample temperature was allowed to cool down to near room temperature by operating the microwave intermittently, and the thermoacoustic signal was recorded with time as the temperature decreased. The samples and transducer were placed in a sealed stainless steel tank. Thermoacoustic signals emitted by sample were coupled to the transducer by oil that is placed in a sealed plastic bag. The actual temperature was also invasively monitored using a digital thermometer as before.

In order to further study the capabilities to detect non-uniform temperature field, measurements were carried out on samples with differing microwave absorption coefficient. A gelatin phantom which measured $10 \times 10 \times 8\,mm^3$ was prepared for the investigation. Amounts of iron oxide (Fe_3O_4) nanoparticles were placed in the centre of the phantom to amplify the temperature gradient when heating. Magnetic nanoparticles can convert the absorbed microwave energy to thermal energy under alternating magnetic fields, which adds the advantage of site-specific targeted temperature rise. The Fe_3O_4 particle is the clinically used absorber for microwave thermotherapy, it can control the microwave energy to the predominated region, effectively decreasing the thermal diffusion and reducing the damage to normal tissue [34–36].

Results

The Grüneisen parameter of water and peak values of thermoacoustic signal versus temperature are presented in Figure 2. A linear relationship between the temperature and the thermoacoustic signal was observed. The circles seen in the figure show how the Grüneisen parameter of water varies with temperature. For water in this temperature range, the Grüneisen parameter is a linear function of temperature, and an increment of 84% was observed in the range of 28–58°C. The fitting curves of $P_{max}(T)$ in the experiment coincide well with the thermal parameters given by Shah et al. [31]. The change rate of Γ provided by the reference is approximately 3.29% per 1°C whereas the estimated dependence of the thermoacoustic signal amplitude rise on temperature is 2.93% per 1°C. Therefore, the change rate of the thermoacoustic signal value with temperature is agreed to be effectively related to the change rate of Γ. The deviations observed can be explained with the temporal variations in microwave pulse energy and detector sensitivity.

A comparison between the thermoacoustic approach and ultrasound methods was made. Temporal wave forms of thermoacoustic signals were extracted and shown in Figure 3. Waves in the figure correspond to thermoacoustic signals that recorded at different temperatures. As shown in the figure, the peak value at 21°C is 172 while it changes to 463 when the temperature increase to 71.5°C, reflecting a calculated change rate of 3.35%/°C. In contrast, the exact travel time change of acoustic is 0.165 μs with the change rate of 2.5‰/°C. The present method increased the

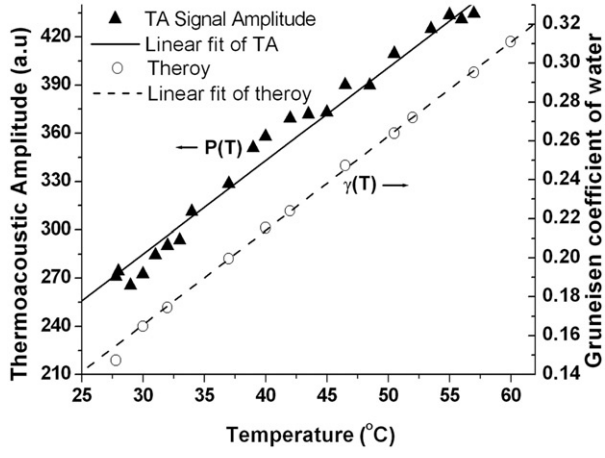

Figure 2. Peak thermoacoustic pressure induced in water with various temperatures. The triangle represents experimental data and the circles are the Grüneisen coefficient. The solid line is the fitting curve of experimental data versus temperature while the dashed line is a fit to literature data [31].

temperature sensitivity by more than an 13.4 times greater than ultrasound method.

The experiments described above reveal a definite relationship between thermoacoustic signal amplitude and temperature of water, while the acoustic can be induced as long as the capacity exists for microwave absorption. Three independent experiments were performed on ex vivo tissues; the corresponding PRF was 15 Hz, 25 Hz and 35 Hz, respectively. Figure 4A, B and C show the peak–peak value of thermoacoustic signal induced in pork muscle at different temperatures. As seen from these figures, signal magnitudes have a linear relationship with temperature in the measured range. In Figure 4A, the linear fit line outcomes match the recorded data with an R^2 of 0.985. In Figure 4B and C, similar results display that the linear curve fitting again matches well with goodness of 0.994 and 0.989. Significant increases of the thermoacoustic amplitudes were observed in all the three experiments, with increasing rate of 2.07%/°C, 1.79%/°C and 1.99%/°C, respectively. The variance may be ruled out by improving the SNR. In microwave thermotherapy, the tumour was generally heated from 37°C to approximately 45°C, and thermoacoustic signals magnitude has an increase of 15% as calculated from Figure 4B and C, which is sensitive

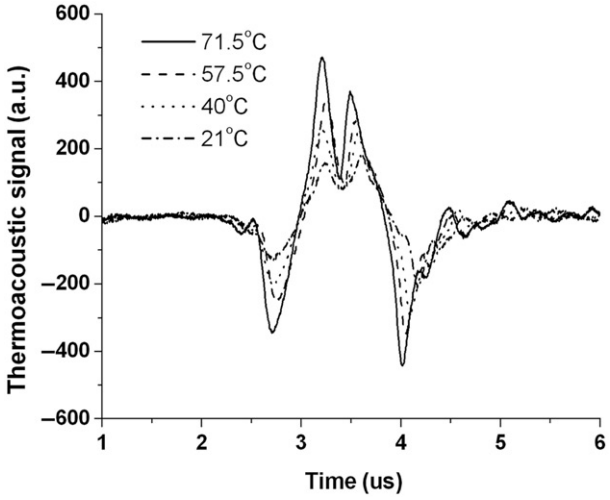

Figure 3. Waveforms of the microwave-induced acoustic pressure for water at various temperatures.

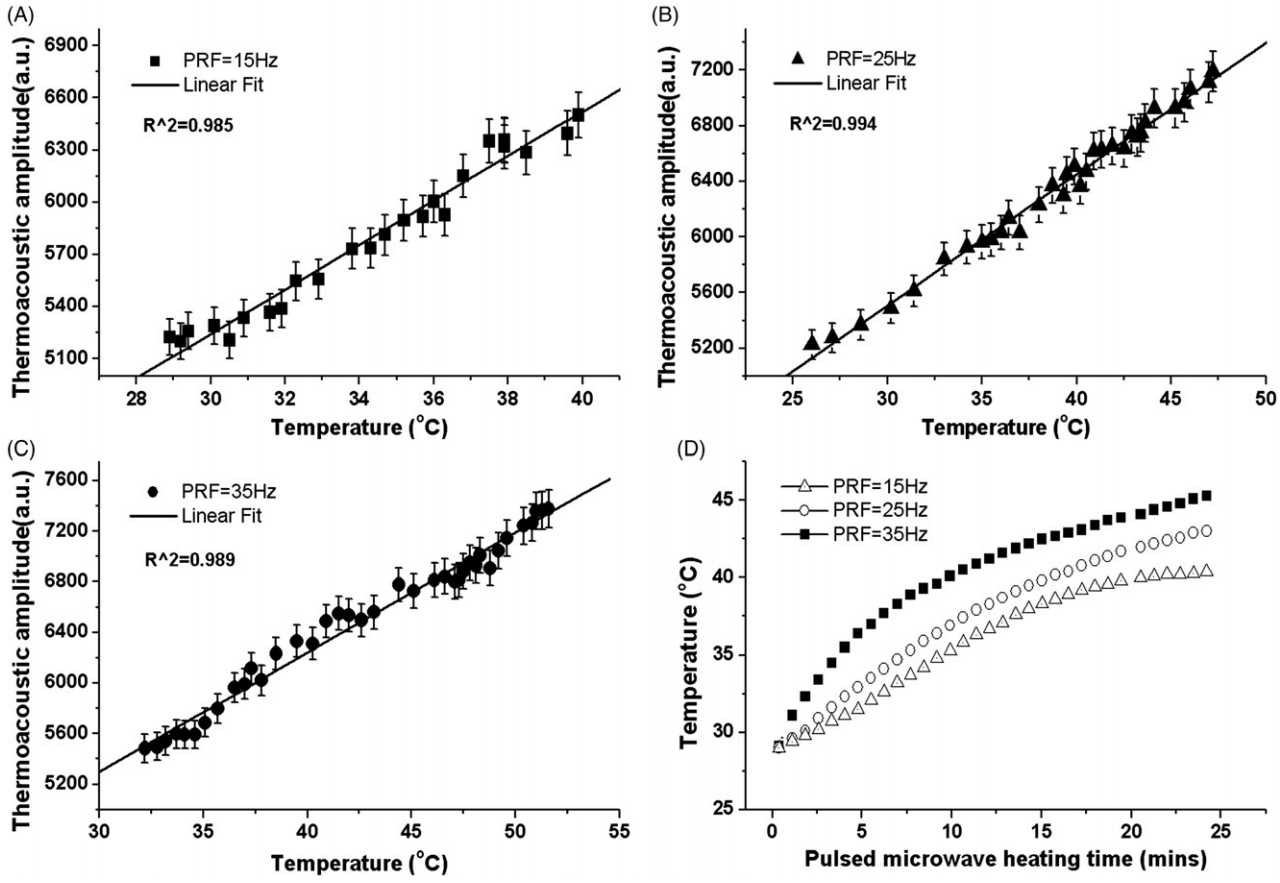

Figure 4. (A, B and C) Dependence of the thermoacoustic pressure on the temperature, which shows goodness fit for linear regression. The test sample was freshly excised pork liver. The PRF is 15 Hz, 25 Hz, 35 Hz, respectively. R^2, goodness of fit. (D) Relationship between the rise of temperatures in ex vivo tissue and the pulse repetition frequency. The average power corresponding to the used PRF is 2.7 W, 4.5 W and 6.3 W respectively.

and reliable to use for treatment monitoring of microwave thermotherapy.

In order to confirm the heating ability of the pulsed microwave, ex vivo muscular tissue was heated by regulating the PRF, while temperatures were recorded by thermometer simultaneously. The consuming time of heating process is shown in Figure 4D. The temperature generally increases with heating time, while it has some difference as the PRF is varied from 15 Hz to 35 Hz. The temperature increased rapidly to 38°C when the PRF is 15 Hz. However, it is much harder to achieve higher temperatures due to heat exchange between tissue and surrounding medium increases with the temperature gradient. Meanwhile, the tissue can be heated up to 50°C when a PRF of 35 Hz was used, and 25 minutes was consumed for the temperature increase from 30°C to 45°C. However, employing higher PRF can eventually give a much more rapid temperature rise. In tumour treatment, damage from microwaves was related to the total dose or energy deposition. Previous experiments (Trevithick et al., 1998) have investigated the effects of different peak power and pulse durations to tumour damage. Experiments indicated that pulsed exposure caused more damage than continuous wave (CW) exposure when given at the same average power and for identical times and temperatures [37]. In a word, the use of pulsed microwave heating for thermotherapy treatment of tumours is a practical and feasible approach.

The actual temperature corresponding to the thermoacoustic signal shown in Figure 4 can be calculated from the linear fit equation. This is shown in Figure 5 and is compared with the temperature recorded by digital thermometer. The actual values are from 27.6°C to 48°C, and the averaged recorded interval is 0.48°C. Thermoacoustic signals detected by transducer was averaged 256 times in one measurement, error bars were added according to the three experiments showed in Figure 4. The calculated results are found to have a better match with data measured by thermometer, the mean differences between them is only 0.767°C. Errors which were induced by microwave fluctuation can be ruled out as the measurements were repeated more times. The measurement precision can be calculated by the change rate of thermoacoustic pressure and corresponding temperature change. As seen from Figure 4, the excited thermoacoustic signals amplitude are approximately 5000 arbitrary units (a.u.) at 30°C, assuming change of 10 a.u. can be detected, which gives us a temperature resolution of 0.2°C. However, temperature resolution can be improved by improving the stability of the microwave pulse energy and employing higher sensitivity transducer. Furthermore, temperature resolution can be increased by averaging several thermoacoustic signals to improve the SNR.

Thermoacoustic imaging has a spatial resolution of sub-mm level, thus temperature change of different points can also be detected by time-resolved one dimensional thermoacoustic signals. Figure 6 shows signal magnitudes induced in phantoms with PRF of 35 Hz. In the figure, the curves marked with A and B are produced by the boundary of the phantom and Fe_3O_4 nanoparticles, respectively. Both of them increase about 50% after 17 minutes of heating. At the beginning of measurements, signal magnitude of Fe_3O_4 particles is 1.33 times larger than that of

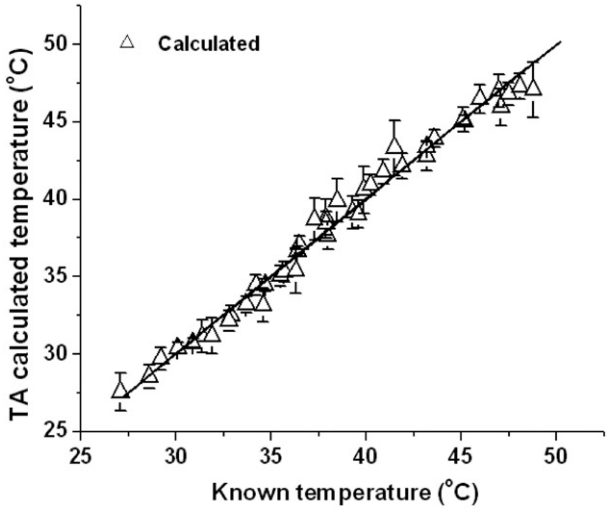

Figure 5. The calculated values (triangle) from thermoacoustic signals versus actual temperature recorded by a digital thermometer. The solid line represents the line of unity.

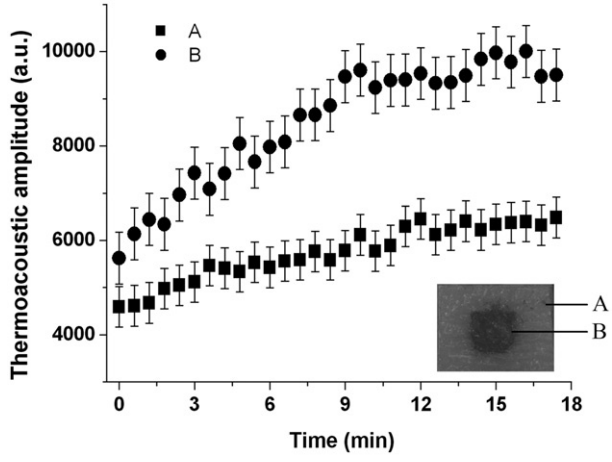

Figure 6. Pulsed microwave-induced acoustic pressure versus heating time with a pulse repetition frequency of 35 Hz. The inset image shows a sample made of agar and Fe_3O_4 particles.

phantom boundary while the difference amplified to 1.54 times after heating, which indicates that the Fe_3O_4 particles give rise to a larger temperature increase in the heating process. These results demonstrate the success of our measurement approach in measuring temperature at different positions with time-resolved one-dimension signals. Moreover, this tool provides an alternative method for reconstructing non-uniform temperature field.

Discussions

Thermotherapy can be carried out on tumours at a depth of a few cm by selecting appropriate microwave wavelength. The temperature distribution is also non-uniform in depth direction due to microwave attenuation, which can be obtained by shifting the focus layer of transducer. (The slice distinguishing ability of the system has been proved by our previous work [33]). The penetration depth of microwaves is related to the microwave wavelength and absorption coefficient of the sample. At the frequency of our experimental set-up, 6 GHz, the penetration depths for fat and muscle are 5.2 cm and 0.7 cm, respectively. Much lower frequency microwaves can have a higher penetration depth.

Compared with continuous wave irradiation, pulsed microwave as a thermotherapy source is especially suitable for the treatment of deep inflammation, since it enhances the penetration depth and treatment effect, causing greater damage to tumours [37]. We propose a combined system for pulsed microwave thermotherapy and temperature monitoring. The power setting would be varied from 50 to 150 W in clinical thermotherapy, and the treatment duration varied from 2 to 20 minutes. To meet the needs of clinical application, the output power of the pulsed microwave system can be controlled under 100 W through an external trigger source. Furthermore, the waveguide can be replaced by an irradiation antenna to focus the microwave on a specific range.

As the system reaches the clinical phase, it is also important to accurately assess the potential safety hazards to patients. A common technique for assessing safety levels for microwave exposure is by characterising specific absorption rates (SAR) inside the body and comparing them to prescribed maximum limits, such as those described by the Institute of Electrical and Electronic Engineers (IEEE) and the International Commission on Non-Ionising Radiation Protection (ICNIRP). The rate of microwave energy deposition or SAR in the lens is related but not identical to the elevation of lens temperature during exposure [37]. According to a study of Trevithick et al. [37] the SAR values for 600 KW peak power pulses sufficient to cause damage at the 10 μm level (SAR 0.01 W/kg) and 20 μm level (SAR 0.28 W/kg) are both below the threshold of 0.4 W/kg assumed in the accepted safety standard of 4 W/kg (this includes the factor of 10 usually used for safety above the minimum biological effect). Further experiments should be conducted to insure the thermotherapy ability of pulsed microwave. Moreover, the magnetic particles can be distributed in very small portions within the targeted area, thus enabling the generation of a precise SAR distribution, which may significantly improve the steering of a thermal therapy compared to conventional hyperthermia techniques [38]. Besides microwave, thermotherapy source can also be high intensity focus ultrasound (HIFU) [39], or laser and radial frequency electromagnetic waves. We predict that if a source is pulsed which can be absorbed by tissue, thermal acoustics can be excited consequently. Therefore the detection method can be widely expanded to other forms of thermotherapy.

The experiments presented in this paper were taken in phantoms and excised tissue, however, heating effects will be somewhat different as applying these procedures to living tissue. The next step in developing and evaluating this combined therapy/monitoring system will be applied to animals in vivo. The volume expansion coefficient and the speed of sound are linearly proportional to temperature up to 55°C [31, 32] which is lower than the temperature of thermal ablation. Hence this approach may fail to provide accurate results for the temperature monitoring of thermal ablation process. However, thermal ablation of tumour tissue is associated with a decrease in water content and conductivity, and thermoacoustic imaging can be used to differentiate thermal lesions from normal tissue [40].

The present method shows the ability of point temperature measurement, however, thermoacoustic imaging is needed to reconstruct a non-uniform temperature field. Speed of data acquisition and image processing remains a challenge as well. More experiments should be carried out to improve real-time temperature field reconstruction capability using the 64-channel parallel data acquisition system: this is ongoing work at our facility.

Conclusions

We have successfully integrated a pulsed microwave for thermotherapy with thermal-induced acoustic for non-invasive temperature monitoring. Preliminary studies on phantoms and ex vivo tissues show that the thermoacoustic pressure indeed varies with temperature, and that the system is sufficiently sensitive to capture these variations. Specifically,

temperature accuracy is better than 0.2°C in the experiments performed here. In addition, the approach has the ability of non-uniform temperature measurement. Therefore, we conclude that the thermoacoustic method has the ability of real-time in situ temperature monitoring during heating. Although more studies should be done to demonstrate the possibilities for applications in clinical biomedicine, clearly it has great potential to yield an integrated system combining thermotherapy with temperature monitoring, which may be developed into valuable real-time feed-back modality for clinical thermotherapy.

Acknowledgements

The authors thank Drs. Liangzhong Xiang, Liming Nie, and Sihua Yang for the help of discussion and experiment, and John Pinar for the help of manuscript writing.

Declaration of interest: This research is supported by the National Basic Research Program of China (2010CB732602), the Program for Changjiang Scholars and Innovative Research Team in University (IRT0829), the National Natural Science Foundation of China (30627003; 30870676), and the Natural Science Foundation of Guangdong Province (7117865).

References

1. Hoffman RM, Monga M, Elliot SP, Macdonald R, Wilt TJ. Microwave thermotherapy for benign prostatic hyperplasia. Cochrane Database Sys Rev 2007;4:1–25.
2. Huston TL, Simmons RM. Ablative therapies for the treatment of malignant diseases of the breast. Am J Surg 2005;189:694–701.
3. Falk MH, Issels RD. Hyperthermia in oncology. Int J Hyperthermia 2001;17:1–18.
4. Nikfarjam M, Christophi C. Interstitial laser thermotherapy for liver tumors. Br J Surg 2003;90:1033–1047.
5. Huang Y, Hu B, Liu D, Liu SJ, Shen E, Wu R. Measuring urethral tissue heat injury temperature of healthy male rabbits during interstitial radiofrequency ablation. Int J Hyperthermia 2009;25:56–64.
6. Volg TJ, Eichler K, Straub R, Engelmann K, Zangos S, Woitaschek D. Laser-induce thermotherapy of malignant liver tumors: General principle, equipment, procedure-side effects, complications and results. Euro J Ultrasound 2001;13: 117–127.
7. Mertyna P, Dewhirst MW, Halpern E, Goldberg W, Goldberg SN. Radiofrequency ablation: The effect of distance and baseline temperature on thermal dose required for coagulation. Int J Hyperthermia 2008;24:550–559.
8. Meaney PM, Zhou T, Fanning MW, Geimer SD, Paulsen KD. Microwave thermal imaging of scanned focused ultrasound heating: Phantom results. Int J Hyperthermia 2008;24:523–536.
9. Nadobny J, Wlodarczyk W, Westhoff L, Gellermann J, Felix R, Wust P. A clinical water-coated antenna applicator for MR-controlled deep-body hyperthermia: A comparison of calculated and measured 3-D temperature data sets. IEEE T Bio-Med Eng 2005;52:505–519.
10. Hiltawsky KM, Kruger M, Starke C, Heuser L, Ermert H, Jensen A. Freehand ultrasound elastography of breast lesions: Clinical results. Ultrasound Med Biol 2001;27: 1461–1469.
11. Fromageau J, Brusseau E, Vray D, Gimenez G, Delachartre P. Characterization of PVA cryogel for intravascular ultrasound elasticity imaging. IEEE Trans Ultrason Ferroelect Freq Contr 2003;50:1318–1324.
12. Bevan PD, Sherar MD. B scan ultrasound imaging of thermal coagulation in bovine liver: Log envelope slope attenuation mapping. Ultrasound Med Biol 2001;27:379–387.
13. Proctor MR, Black PM. Minimally Invasive Neurosurgery. Totowa, NY: Humana Press; 2005.
14. Worthington AE, Trachtenberg J, Sherar MD. Ultrasound properties of human prostate tissue during heating. Ultrasound Med Biol 2002;10:1311–1318.
15. Arthur RM, Straube WL, Trobaugh JW, Moros EG. In vivo change in ultrasonic backscattered energy with temperature in motion-compensated images. Int J Hyperthermia 2008;24: 389–398.
16. Arthur RM, Straube WL, Trobaugh JW, Moros EG. Non-invasive estimation of hyperthermia temperatures with ultrasound. Int J Hyperthermia 2005;21:589–600.
17. Clarke RL, Bush NL, Haar GR. The changes in acoustic attenuation due to in vitro heating. Ultrasound Med Biol 2003;29:127–135.
18. Ku G, Wang LV. Scanning microwave-induced thermoacoustic tomography: Signal, resolution, and contrast. Med Phys 2001;28:4–10.
19. Kruger RA, Miller KD, Reynolds HE, Kiser WL, Reinecke DR, Kruger GA. Contrast enhancement of breast cancer in vivo using thermoacoustic CT at 434 MHz. Radiology 2000;216:279–283.
20. Tam AC. Application of photoacoustic sensing techniques. Rev Mod Phys 1986;58:381–431.
21. Calasso IG, Craig W, Diebold GJ. Photoacoustic point source. Phys Rev Lett 2001;86:3550–3553.
22. Guo B, Li J, Zmuda H, Sheplak M. Multifrequency microwave-induced thermal acoustic imaging for breast cancer detection. IEEE Trans Bio Eng 2007;54:2000–2010.
23. Larina IV, Larin KV, Esenaliev RO. Real-time optoacoustic monitoring of temperature in tissues. J Phys D: Appl Phys 2005;38:2633–2639.
24. Sigrist MW. Laser generated acoustic waves in liquids and solids. J Appl Phys 1986;60:83–122.
25. Oraevsky AA, Jacques SL, Tittel FK. Measurement of tissue optical properties by time-resolved detection of laser-induced transient stress. Appl Opt 1997;36:402–415.
26. Xu Y, Wang LV, Ambartsoumian G, Kuchment P. Reconstructions in limited-view thermoacoustic tomography. Med Phys 2004;31:724–733.
27. Yuan Z, Jiang HB. Quantitative photoacoustic tomography: Recovery of optical absorption coefficient maps of heterogeneous media. Appl Phys Lett 2006;88:231101–231103.
28. Xu MH, Wang LV. Pulsed-microwave-induced thermoacoustic tomography: Filtered backprojection in a circular measurement configuration. Med Phys 2002;29:1661–1669.
29. Koughia C, Kasap S, Capper P. Springer Handbook of Electronic and Photonic Materials. Springer Verlag; 2006.
30. Wakako A, Tadaharu A, Akihiko Y. Thermal stress analysis of thermoviscoelastic hollow cylinder with temperature-dependent thermal properties. J Therm Stresses 2005;28: 29–46.
31. Shah J, Park S, Aglyamov S, Larson T, Ma L, Sokolov K, Johnston K, Milner TS, Emelianov Y. Photoacoustic imaging

and temperature measurement for photothermal cancer therapy. J Biomed Opt 2008;13:1–13.
32. Duck F. Physical Properties of Tissue: A Comprehensive Reference Book. New York: Academic Press; 1990. pp 167–223.
33. Nie LM, Xing D, Yang SH. In vivo detection and imaging of low-density foreign body with microwave-induced thermo-acoustic tomography. Med Phys 2009;36:3429–3437.
34. Thiesen B, Jordan A. Clinical applications of magnetic nanoparticles for hyperthermia. Int J Hyperthermia 2008;24: 467–474.
35. Zhao DL, Zhang HL, Zeng XW, Xia QS, Tang JT. Inductive heat property of Fe3O4/polymer composite nanoparticles in an ac magnetic field for localized hyperthermia. Biomed Mater 2006;1:198–201.
36. Salloum M, Ma R, Zhu L. Enhancement in treatment planning for magnetic nanoparticle hyperthermia: Optimization of the heat absorption pattern. Int J Hyperthermia 2009;25:309–321.
37. Trevithick JR, Creighton MO, Sanwal M, Baskerville JC, Bassen HI, Brown DO. In vitro lenticular effect enhancement by L-band pulsed VS continuous wave micro-wave irradiation of rat lens. Scanning Microscopy 1998;12:609–629.
38. Barry SE. Challenges in the development of magnetic particles for therapeutic applications. Int J Hyperthermia 2008;24: 451–466.
39. O'Neill BE, Li KC. Augmentation of targeted delivery with pulsed high intensity focused ultrasound. Int J Hyperthermia 2008;24:506–520.
40. Jin X, Xu Y, Wang LH. Imaging of high-intensity focused ultrasound-induced lesions in soft tissue using thermoacoustic tomography. Medical Physics 2005;32:5–11.